Evaluation of Optimal Covariance Models for EKF-based Wheeled Mobile Robot Localization

Imre Kovacs[1*], Massimo Stefanoni[2], Richard Pesti[1], Dominik Csik[1], Peter Sarcevic[1] and Ákos Odry[1]

[1] Department of Mechatronics and Automation, Faculty of Engineering, University of Szeged, Mars tér 7, H-6724 Szeged, Hungary, {kovacs.imre, pestir, csikd, sarcevic, odrya}@mk.u-szeged.hu

[2] Doctoral School of Applied Informatics and Applied Mathematics, Obuda University, Bécsi 96/B, H-1034 Budapest, Hungary, massimo.stefanoni@uni-obuda.hu

Abstract: Accurate and reliable localization is a key requirement in autonomous mobile robotics. The performance of EKF-based localization is highly dependent on the proper configuration of its process and measurement noise covariance matrices. This paper investigates the optimization of an Extended Kalman Filter (EKF)-based localization framework through three covariance tuning strategies, using Particle Swarm Optimization (PSO). The study focuses on the fusion of odometry and Absolute Positioning System (APS) measurements for successful localization of a wheeled mobile robot performing trajectory tracking. The first strategy optimizes the diagonal elements of the EKF's process and measurement noise covariance matrices (R and Q), while the second method tunes motion model coefficients (α_1 and α_2) that govern uncertainty propagation from encoder data. The third approach introduces an adaptive model where angular velocity – measured by a gyroscope – is used to dynamically adjust these coefficients. Each method is evaluated on five real-world trajectories across seven fitness modes using RMSE, MAE, and MAXE metrics. Results show that all three strategies outperform the baseline EKF. Among them, the method based on tuning the process and measurement noise covariance matrices delivers the most consistent improvements, while the gyro-adaptive method achieves peak performance in highly dynamic scenarios. However, the latter displays higher variance, motivating future use of nonlinear models for improved robustness. The findings highlight the benefits of optimization-driven and context-aware tuning in enhancing EKF localization performance.

Keywords: robot localization; sensor fusion; EKF; parameter tuning; Particle swarm; mobile robot

1 Introduction

The accurate localization has a fundamental role in robotics, as the applications depend on the robot's ability to determine its absolute position in their environment. There are several engineering applications that use Kalman-Filter (KF) based approaches to achieve suitable localization accuracy, such as precision agriculture [1] [2], autonomous vehicles [3], hospital research [4] or mobile robot systems [5].

Localization approaches are generally categorized into two main types: absolute (or global) localization and relative localization. Global localization refers to the process of determining a robot's position within an environment without any prior knowledge of its starting point. This approach is commonly employed in outdoor or large-scale environments, where external infrastructure such as satellite-based systems, landmarks, or beacons can be leveraged [6-8]. In contrast, relative localization assumes an initially known position and continuously updates the robot's pose based on sensor readings. This method is widely used in structured or indoor environments, where global references are unavailable or unreliable, relying instead on data from onboard sensors such as inertial measurement units (IMUs), wheel encoders, or vision systems [9] [10].

Localization is typically achieved through multi-sensor fusion, where absolute and relative measurements are integrated to estimate the robot's position, pose, and trajectory. One of the most widely used methods for this purpose is the Extended Kalman Filter (EKF), which provides a recursive framework for fusing data from sensors such as wheel encoders, IMUs, LiDARs, and absolute positioning systems (APSs). Several studies have demonstrated the effectiveness of EKF-based fusion techniques in improving localization accuracy across different domains. For example, in [11], an EKF was applied to fuse odometry and ultrasonic positioning data, significantly reducing the average error in indoor environments, achieving below 10 cm average position error. In [12], a fusion is proposed between RSSI and Phase Shifting data, by a KF, which leads the authors to get a position error less than 6.6 cm. Advanced variants such as the Taylor expansion-based EKF (TEKF) [13] and the Unscented Kalman Filter (UKF) [14] [15] have been proposed to address the linearization limitations of traditional EKFs. These techniques demonstrated better handling of non-linear dynamics and higher robustness in sensor-degraded scenarios. In [16], the authors proposed a system that uses UKF to achieve around 10% less position error than a regular KF.

Although EKF-based fusion is widely adopted, the accuracy of such systems is strongly influenced by the configuration of the noise covariance matrices $\boldsymbol{R}$ (process noise) and $\boldsymbol{Q}$ (measurement noise). Inappropriate tuning of these matrices can lead to filter divergence or degraded accuracy. Traditionally, these parameters are either set heuristically or manually tuned, based on prior experiments. However, this process is often time-consuming, suboptimal, and not generalizable across different environments or robot platforms [17]. To address this challenge, recent research has

explored the application of optimization algorithms to automatically identify optimal or near-optimal values for $\boldsymbol{R}$ and $\boldsymbol{Q}$. Among these methods, Particle Swarm Optimization (PSO) has gained attention due to its global search capabilities and ease of implementation. For instance, PSO has been applied to optimize filter parameters for autonomous vehicle path planning [18], AUV navigation [19], and a SLAM application for Forward-Looking Sonar [20] or for an RGB-D Camera-based system [21]. These applications consistently outperform static or manually tuned EKF configurations.

This paper focuses on the global optimization of the noise parameters in EKF-based localization systems using PSO. In contrast to a previous study [22] that primarily investigated the impact of varying the update frequency and measurement noise levels of APS, this work assumes fixed update rates and noise characteristics, thereby isolating and analyzing the effect of EKF parameter tuning on localization performance. The proposed methodology evaluates three distinct optimization strategies. First, the diagonal elements of the process noise covariance matrix $\boldsymbol{R}$ and the measurement noise covariance matrix $\boldsymbol{Q}$ are optimized independently to identify their most effective configuration for each trajectory and evaluation mode. Second, the parameters α_1 and α_2, which govern the propagation of uncertainty from wheel encoder measurements in the motion model, are adjusted to better represent motion-induced noise within the prediction step of the EKF. Finally, the third scenario introduces a more advanced, adaptive formulation in which gyroscopic measurements are incorporated to dynamically modulate the control noise parameters, effectively linking angular velocity to model uncertainty. This gyro-based extension allows the filter to respond to environmental and kinematic variations in real-time, enhancing robustness in dynamic or uneven terrain. The performance of each optimization strategy is systematically assessed across five distinct real-world trajectories using seven evaluation metrics based on Root Mean Square Error (RMSE), Mean Absolute Error (MAE), Maximum Error (MAXE), and their combinations. The experimental results confirm that all three approaches contribute to measurable improvements in localization accuracy, demonstrating the benefits of data-driven, scenario-specific tuning of EKF parameters in multi-sensor fusion frameworks.

The rest of this paper is organized as follows**.** Section 2 describes the simulation setup, including the reference trajectories, the fitness functions, and the evaluation metrics briefly introduces the EKF framework used in this study and presents the PSO strategies applied to optimize the filter parameters. Section 3 presents the obtained results and analyses the improvements in localization accuracy under different optimization scenarios. Finally, Section 4 concludes the paper and outlines directions for future work.

2 Methodological Framework

2.1 Experimental Setup and Trajectory Data

The 2D localization performance is evaluated on a differential drive wheeled robot that follows five predefined real-world trajectories (Track 1-5). The robot is equipped with incremental wheel encoders, and during each experimental run, the encoder readings are recorded to simulate odometry. These encoder-derived trajectories serve as the baseline for localization, which is then enhanced using EKF-based sensor fusion with APS measurements.

To ensure controlled experimentation, the APS coordinates are not derived from real sensors but are artificially generated using ground truth data. The generation process comprises two stages: selection and perturbation. In the selection phase, APS updates are sampled at a fixed frequency of 1 Hz from the ground truth path. In the perturbation phase, zero-mean Gaussian noise with a standard deviation of 60mm is added to the coordinates. This simulates realistic APS noise under consistent conditions across all trajectories. The details of this experimental setup are described in [22].

Figure 2 illustrates a) the differential drive robot equipped with wheel encoders and b) a representative test track layout recorded during experimentation while Figure 2 depicts the five reference trajectories used in the evaluation,

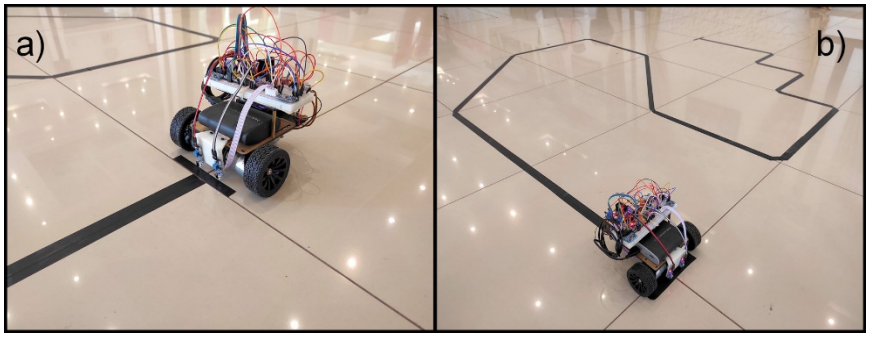

Figure 1

a) The differential drive mobile robot used in the experiments.
b) A snapshot of one of the predefined test tracks during deployment.

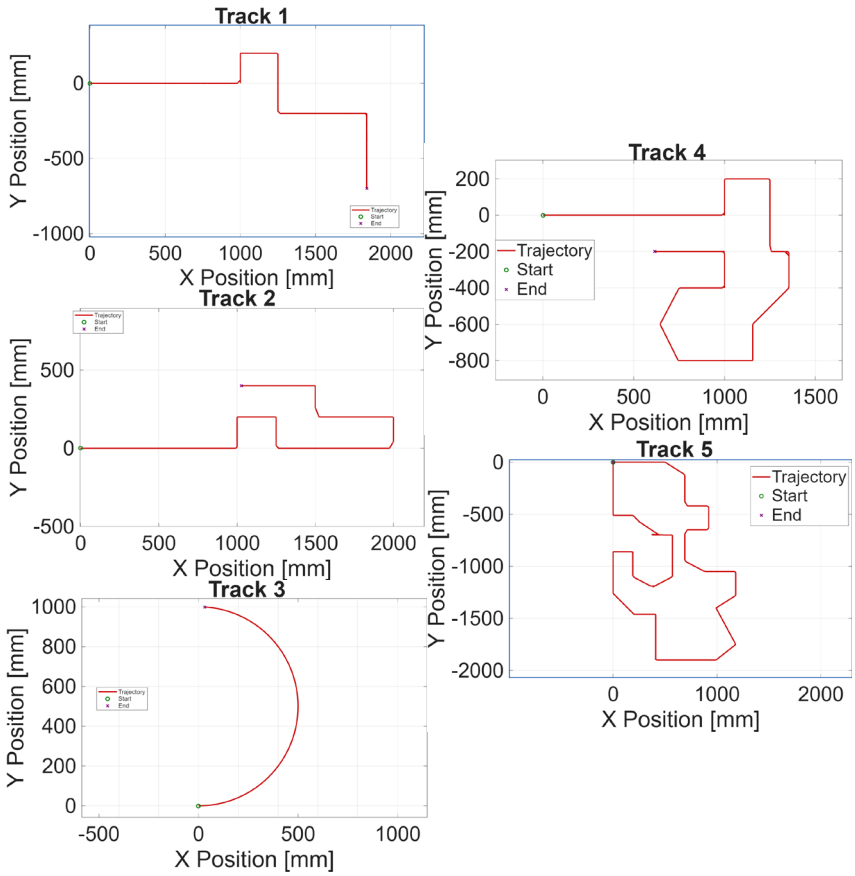

Figure 2
Example trajectories used during the experimental evaluation

2.2 The EKF Framework

The EKF framework adopted in this study builds upon the methodology detailed in [22], offering a reliable and well-established basis for multi-sensor data fusion. The filter operates in two iterative steps: the prediction phase estimates the robot's next state using motion inputs derived from wheel encoder data, while the update phase incorporates simulated APS observations to correct this estimate. The APS updates are provided at a fixed frequency of 1 Hz, and Gaussian noise with a standard deviation of 60 mm, is consistently applied across all scenarios, to model real-world measurement uncertainty.

Unlike previous studies focusing on alternative sensor fusion approaches or varying APS characteristics, this work retains a fixed measurement frequency and noise

profile to isolate and investigate the effects of different noise parameter tuning strategies. The EKF implementation is not re-derived here, as its mathematical formulation – including state propagation, covariance prediction, Kalman gain calculation, and state correction – is directly based on the formulation presented in [22]. By maintaining a consistent filtering architecture, the study can focus exclusively on the effect of parameter tuning via PSO. This enables the evaluation of how different noise model configurations influence localization accuracy, independent of external sensor variability or changes in filter design.

2.3 Optimization Strategies

To enhance the localization accuracy of the EKF-based sensor fusion system, three distinct optimization strategies were developed, each leveraging the global search capabilities of Particle Swarm Optimization (PSO). These strategies target different components of the noise modelling process within the EKF framework and are designed to explore how data-driven tuning can improve performance under fixed sensing conditions.

2.3.1 R and Q Diagonal Elements Optimization

In the first strategy, the focus is placed on directly tuning the noise covariance matrices of the EKF. These matrices – $\boldsymbol{R} \in \mathbb{R}^{3x3}$ representing the process noise, and $\boldsymbol{Q} \in \mathbb{R}^{2x2}$ representing the measurement noise – play a critical role in the filter's ability to accurately estimate the robot's position. Improper settings can lead to significant drift or instability in the state estimation. Despite their importance, these parameters are often manually tuned or kept constant across different environments and robots, which reduces adaptability and generalization. To overcome this limitation, the elements of both matrices are treated as optimization variables. Assuming diagonal structure for both $\boldsymbol{R}$ and $\boldsymbol{Q}$, the optimization targets five variables:

$$\boldsymbol{R} = diag(r_1, r_2, r_3) \tag{1}$$

$$\boldsymbol{Q} = diag(q_1, q_2) \tag{1}$$

The five variables are constrained by the following search bounds: $r_1, r_2 \in [1, 10^5]$, $r_3 \in [10^{-6}, 1]$, $q_1, q_2 \in [10, 10^4]$. These ranges were selected to balance flexibility and numerical stability. The PSO algorithm is configured with 50 particles and runs for 150 iterations. To ensure statistical reliability and avoid bias due to initial swarm configurations, 20 independent seeds are used in each case. The optimization is carried out over five distinct tracks and seven evaluation modes, which include RMSE, MAE, MAXE, and weighted combinations of these error metrics.

Although the APS updates are generated using a fixed Gaussian noise model with a standard deviation of 60 mm, the decision to include the $\boldsymbol{Q}$ matrix in the optimization process was motivated by practical considerations. In real-world systems, sensor noise characteristics are often only approximately known or can vary due to environmental interference, sensor aging, or imperfect calibration. Therefore, optimizing $\boldsymbol{Q}$ allows the system to account for these uncertainties implicitly, potentially improving robustness and generalization.

This method provides a globally optimal EKF configuration per track and objective function, under fixed APS conditions. By evaluating the performance across multiple tracks and fitness metrics, this strategy serves as a baseline for comparison with more advanced methods.

2.3.2 Motion Model Coefficients Optimization

In this approach, rather than optimizing the entire noise covariance matrices, the focus shifts to tuning two scalar coefficients – α_1 and α_2 – that directly influence the control noise modelling in the EKF's prediction step. These coefficients are embedded in the noise formulation of the odometry-based motion model and affect how translational and rotational uncertainties are quantified based on encoder readings.

In the EKF formulation, the variances σ_l^2 and σ_r^2 of the control noise for the left and right wheels are defined as [22]:

$$\sigma_l^2 = (\alpha_1 l)^2 + (\alpha_2 (l - r))^2 \tag{3}$$

$$\sigma_r^2 = (\alpha_1 r)^2 + (\alpha_2 (l - r))^2 \tag{4}$$

Where, l and r denotes the distances travelled respectively by the left and right wheels between two consecutive time stamps. The α_1 and α_2 account for uncertainty caused by the translational and differential motion.

These variances are then used to construct the process noise covariance matrix $\boldsymbol{R}$ in the EKF prediction step. Specifically, the EKF models the control noise in the space of linear and angular velocities, requiring a transformation from the wheel-space variances into the robot's motion model. This is achieved through the Jacobian-based propagation:

$$\boldsymbol{R} = \boldsymbol{V} \cdot diag(\sigma_l^2, \sigma_r^2) \cdot \boldsymbol{V^T} \tag{5}$$

where **V** is the Jacobian is the Jacobian of the motion model with respect to the control inputs. The $\boldsymbol{Q}$ matrix in this scenario is fixed as $\boldsymbol{Q} = diag(60^2, 60^2)$, corresponding to the known APS standard deviation of 60mm.

The PSO algorithm is tasked with identifying the optimal pairs of the two parameters within the bounded search space $\alpha_1, \alpha_2 \in [0,1]$, and the optimization parameters – such as particles, iterations and seed – and the fitness function modes are the same as in 1), ensuring consistency with the other optimization strategies.

This method offers a compact parameter space while directly targeting a critical component of the filter – the propagation of uncertainty – thereby enabling efficient tuning of motion model fidelity without altering the full covariance structure.

2.3.3 Adaptive Gyro-Based Noise Modelling

The third optimization strategy introduces adaptivity to the EKF's motion model by incorporating gyroscopic feedback. This approach is motivated by the observation that wheel slip, surface irregularities, and turning maneuvers often correlate with angular velocity. Instead of assuming fixed coefficients for control noise modelling, the filter dynamically adjusts the uncertainty based on real-time sensor input.

The angular velocity ω_z is estimated as the average of two gyroscope measurements from identical IMUs mounted on the robot. This measurement is then used to linearly modulate the control noise parameters as follows:

$$\alpha_1 = a_1 + b_1|\omega_z| \tag{6}$$

$$\alpha_2 = a_2 + b_2|\omega_z| \tag{7}$$

where,

a_1, a_2 are the base noise levels, and b_1, b_2 are scaling coefficients determining the sensitivity to the angular velocity

The PSO algorithm is tasked with optimizing these four parameters (a_1, a_2, b_1, b_2) in the search bound of: $a_1, a_2 \in [0,1]$, and $b_1, b_2 \in [0,5]$. The inclusion of gyro-based adaptivity allows the EKF to respond to motion dynamics in real time, increasing robustness in sharp turns, uneven terrain, or scenarios with abrupt direction changes. The same evaluation methodology is applied: 50 particles, 150 iterations, and 20 random seeds across all five tracks and seven fitness modes.

2.3.4 Optimization Procedure

In all three optimization strategies discussed above, the objective of PSO is to minimize a scalar-valued fitness function that quantifies localization error. Seven optimization modes are defined to guide the fitness evaluation process. Mode 1 minimizes the RMSE, Mode 2 focuses on the MAE, and Mode 3 targets the MAXE. Modes 4 through 7 represent composite metrics combining two or more of these quantities: Mode 4 minimizes the sum of RMSE and MAE, Mode 5 the sum of RMSE and MAXE, Mode 6 the sum of MAE and MAXE, and Mode 7 considers the aggregated sum of all three metrics—RMSE, MAE, and MAXE. These modes enable the optimization to target various aspects of the error distribution, depending on the application-specific priorities (e.g., minimizing average error versus suppressing worst-case deviations). To ensure statistical robustness and minimize the influence of random initialization, each PSO run is repeated across 20 different random seeds. This results in a total of 700 independent optimization runs per

strategy. For each configuration, the best-performing parameter set is retained based on the selected fitness metric.

All experiments and PSO routines are implemented in MATLAB R2025a. The EKF implementation is executed for each particle's parameter configuration to compute the corresponding trajectory and localization error. The simulation setup remains consistent across all trials: the robot starts from the same initial state, the APS operates at a fixed frequency of 1 Hz, and the standard deviation of the simulated APS noise is fixed at 60mm. The optimized parameters derived from PSO are used in the subsequent evaluation phase to assess their impact on localization accuracy across all test tracks and modes. The effectiveness of each strategy is compared in Section III.

3 Experimental Results

This section analyses the localization performance achieved through the three proposed optimization strategies.

Figure 3 presents a heatmap visualization of RMSE improvement percentages achieved by the RQ optimization strategy across seven fitness modes and five trajectory scenarios. Each cell quantifies the relative improvement in RMSE compared to the baseline EKF implementation with fixed parameters. Higher values indicate more effective tuning. The results reveal that optimization consistently leads to notable performance gains, particularly on Tracks 1 through 4. The highest single-mode improvement reaches 48.4% on Track 3 (Mode 2), while several modes demonstrate over 30% average improvement across multiple tracks. Notably, Modes 4-7, which involve composite fitness metrics, tend to yield the most balanced improvements, suggesting their effectiveness in guiding PSO toward globally robust solutions. Track 5, which contains more complex turns and sharp angle transitions, presents the lowest average improvement. This suggests that trajectory complexity poses a challenge for static parameter configurations and highlights the need for adaptive modelling. Figure 4 provides a comparative overview of the overall improvement distributions achieved by each strategy across all tracks and optimization modes. Subfigure a) illustrates the three metrics improvements intervals and means.

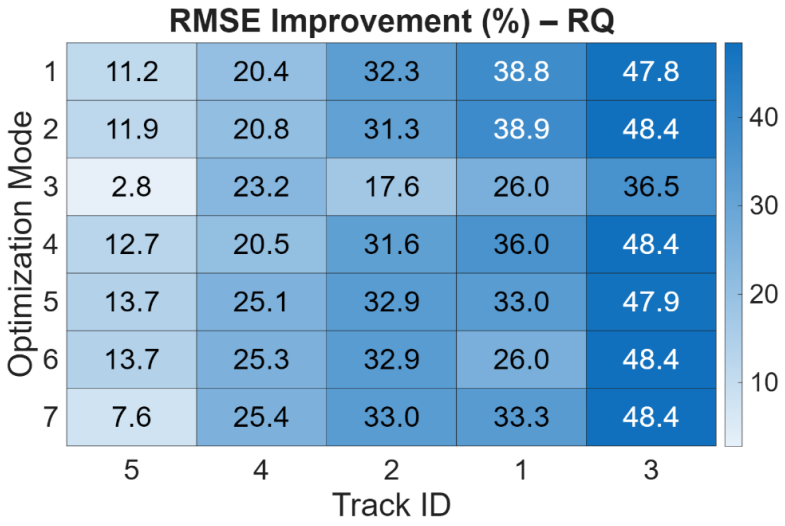

Figure 3
RMSE improvement (%) achieved by RQ optimization strategy

The heatmaps of MAE and MAXE show similar trends. While numerical values slightly vary, the best-performing modes remain consistent, reinforcing the robustness of composite fitness objectives and the general effectiveness of the RQ tuning strategy across error metrics.

The second method shows RMSE improvements comparable to the RQ method, occasionally even surpassing it (e.g., Track 3, Modes 4 and 7). However, some modes exhibit weak or even negative gains, indicating less consistent performance, likely due to data issues or suboptimal convergence. While the gyroscope-based method achieves similar peak improvements to RQ in isolated cases, but overall results are more erratic, with several modes showing negative performance. Despite these shortcomings, the method still demonstrates potential under certain conditions.

Subfigures b) and c) also illustrate the three metrics boxplots, respectively, the first and second methods, exhibit strong median performance with relatively compact interquartile ranges and few negative outliers, confirming their stability. In contrast, the third shows a greater variance and a higher number of outliers, with several instances of performance degradation, especially in MAE and MAXE. These results reinforce earlier observations: while third can be effective under specific conditions, first and second provide more reliable and consistent benefits overall.

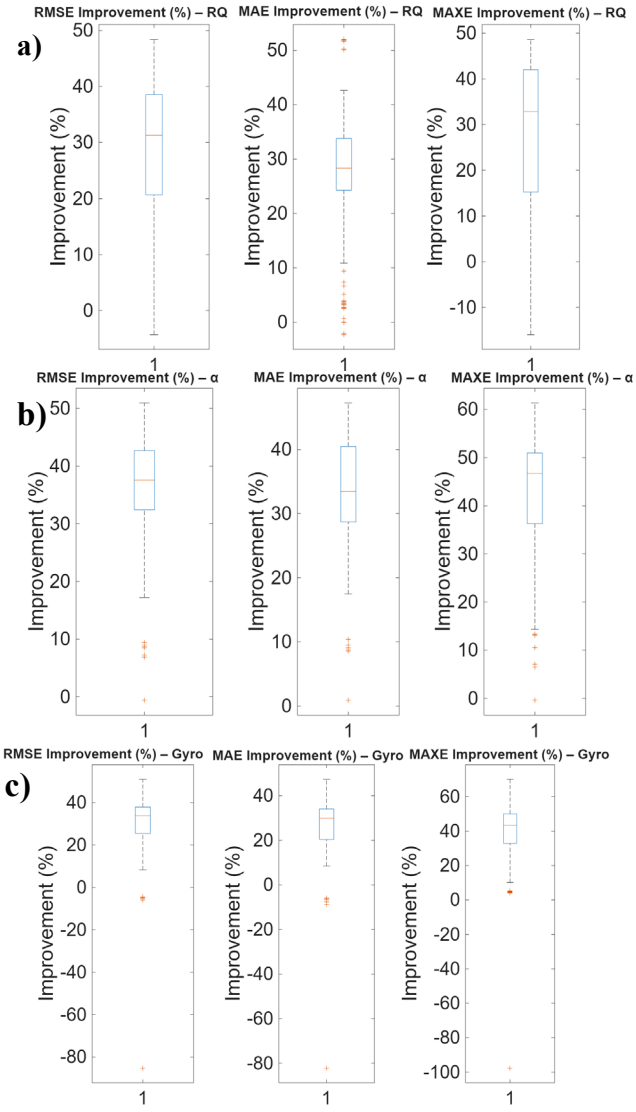

Figure 4
Boxplots of the three investigated methods improvements

To further quantify the performance differences between the methods, Table I summarizes the absolute RMSE values (in meters) obtained on each track using the baseline EKF configuration and the three optimized variants: 1), 2) and 3). The results confirm the earlier observations: all three optimization strategies provide consistent RMSE reductions compared to the original configuration. While

3) achieves the lowest RMSE in several cases – particularly on Tracks 3 and 5 – it does so with higher variance, as previously shown in the boxplots. In contrary, first and second strategies demonstrate more stable improvements across the board. Notably, the second strategy often outperforms first on Tracks 1 and 2, but underperforms on Tracks 3 and 5, highlighting the track-dependent nature of each strategy's effectiveness. To support the visual findings with precise numerical values, Table I reports the absolute RMSE results for each track and optimization mode. These values allow for direct comparison of estimation accuracy between the baseline EKF and each tuning method. The results highlight both the strengths and limitations of the proposed strategies under varying trajectory complexities.

In conclusion, the experimental results clearly demonstrate that all three proposed optimization strategies yield significant improvements in localization accuracy over the baseline EKF configuration. The first method delivers consistently strong results with limited variance, making it a robust general-purpose solution across diverse scenarios. The second strategy often matches or even surpasses the first performance in certain tracks, particularly in early trajectories with smoother dynamics. However, it occasionally exhibits inconsistent results, due to increased sensitivity to convergence behavior or optimization landscape. The third, while capable of achieving the lowest RMSE values in select configurations – especially in more complex scenarios – suffers from higher variability and occasional performance degradation. This instability can be attributed to the dynamic nature of gyro-based adaptation, which, while promising, may require further constraints or context-aware smoothing to ensure reliable performance across all conditions. To address this, future work may consider employing nonlinear or adaptive functions to relate gyro input (e.g., angular velocity) to the process noise parameters. Such models could better capture the relationship between motion dynamics and uncertainty, enabling the filter to respond more effectively to real-world variability.

The comprehensive evaluation – including heatmaps, boxplots, and raw RMSE values – provides convincing evidence that composite fitness modes are more effective at guiding optimization toward globally beneficial configurations. Furthermore, the results reaffirm the importance of matching the filter's internal model to both sensor behavior and environmental characteristics.

Table 1

Summary of the procedure

Track	**Mode**	**Original RMSE [mm]**	**1) RMSE [mm]**	**2) RMSE [mm]**	**3) RMSE [mm]**
1	1	47.8760	29.3130	29.7290	31.7730
	2	47.8760	29.2640	29.9860	32.4480
	3	47.8760	35.4420	34.5650	36.2440
	4	47.8760	30.6320	29.8990	32.1720
	5	47.8760	32.0700	31.6440	33.3160

	6	47.8760	35.4280	30.5910	32.3660
	7	47.8760	31.9510	30.9100	32.0950
2	1	63.0980	42.7160	36.1690	36.4930
	2	63.0980	43.3570	39.1900	38.5080
	3	63.0980	52.0220	34.2000	36.7160
	4	63.0980	43.1390	37.5230	37.1280
	5	63.0980	42.3110	34.0220	34.0120
	6	63.0980	42.3700	33.7810	40.7580
	7	63.0980	42.2830	34.0220	36.4560
3	1	34.8470	18.1820	33.7810	39.3920
	2	34.8470	17.9770	17.7850	17.7760
	3	34.8470	22.1140	28.1600	39.3920
	4	34.8470	17.9940	17.3840	17.3750
	5	34.8470	18.1630	33.7810	39.3920
	6	34.8470	17.9720	33.7810	39.3920
	7	34.8470	17.9810	17.1050	19.8630
4	1	43.2430	34.4180	27.0720	29.1080
	2	43.2430	34.2280	29.2260	29.9610
	3	43.2430	33.2010	29.4050	31.6120
	4	43.2430	34.3970	27.6980	28.8750
	5	43.2430	32.4070	27.3740	39.3920
	6	43.2430	32.3150	29.1840	26.4170
	7	43.2430	32.2660	25.2010	28.6300
5	1	65.1240	57.8260	59.6090	65.8680
	2	65.1240	57.3850	59.2760	63.6290
	3	65.1240	63.3060	33.7810	67.9200
	4	65.1240	56.8600	59.4700	63.9820
	5	65.1240	56.1790	33.7810	68.3180
	6	65.1240	56.1720	33.7810	68.3060
	7	65.1240	60.1470	59.4680	63.6410

To provide a concrete example of the localization behavior, Figure 5 illustrates the estimated trajectories obtained from the baseline EKF and the three optimization strategies on Track 2, alongside the ground truth path. The results clearly show that all optimized methods follow the reference path more closely than the unoptimized baseline. In particular, the first method demonstrates a substantial reduction in drift and deviation throughout the entire trajectory. The second strategy also achieves accurate localization, especially in smooth linear sections. The gyro-based optimization exhibits competitive performance but shows greater deviation during sharp transitions, consistent with the previously reported variability. This visual comparison further supports the quantitative results and highlights the strengths and limitations of each approach.

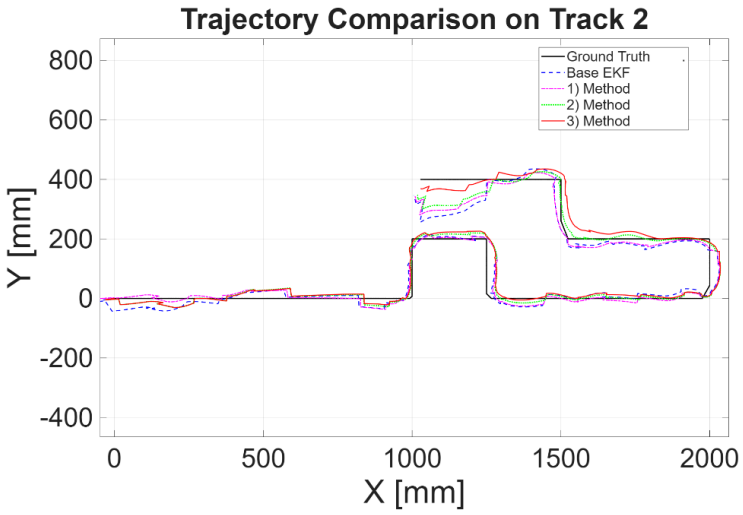

Figure 5
Localization Trajectories on Track 2 Using Different Optimization Strategies

Conclusions

This study presented a comparative evaluation of three PSO-based optimization strategies, to improve the performance of EKF-based localization systems. The following methods were assessed across multiple real-world trajectories, using various fitness metrics:

1) Noise covariance matrix tuning
2) Motion model coefficient tuning
3) Gyro-adaptive control noise modulation

The results consistently showed that all three strategies outperformed the baseline EKF with fixed parameters, delivering measurable improvements in localization accuracy.

Among the methods, the first exhibited the most stable and balanced performance across scenarios, making it a strong general-purpose solution. The second method demonstrated high effectiveness in smoother trajectories but showed sensitivity to track complexity. The third method achieved the lowest RMSE in certain dynamic cases, yet its higher variance highlighted the limitations of using a linear relationship between angular velocity and noise parameters.

To address this, future work will explore nonlinear adaptive models that more accurately capture the relationship between gyroscopic inputs and process noise, thereby enabling the EKF to better adapt to environmental dynamics. Additionally, extending the framework with real-time classification and parameter adjustment

based on terrain or motion characteristics, could further enhance localization robustness.

The findings support the integration of optimization and adaptivity as essential tools in the design of reliable localization systems for mobile robots operating under uncertain and variable conditions.

Acknowledgement

The work was supported by the National Research, Development, and Innovation Fund of Hungary through project no. 142790 under the FK_22 funding scheme.

References

[1] D. Vieira, R. Orjuela, M. Spisser, and M. Basset: Positioning and Attitude determination for Precision Agriculture Robots based on IMU and Two RTK GPSs Sensor Fusion, in IFAC-PapersOnLine, 2022

[2] T. Severin and D. Soffker: Sensor optimization for altitude estimation of spraying drones in vineyards, in IFAC-PapersOnLine, 2022

[3] M. Singh, S. Lakra, S. Das, S. K. Mishra, A. K. Sahoo, and B. Acharya: Extended Kalman Filter-Based Position Estimation in Autonomous Vehicle Applications, in Lecture Notes in Electrical Engineering, 2023

[4] A. Ziegl et al.: MHealth 6-minute walk test - Accuracy for detecting clinically relevant differences in heart failure patients, in Proceedings of the Annual International Conference of the IEEE Engineering in Medicine and Biology Society, EMBS, 2021

[5] M. Stefanoni, M. Takács, Á. Odry, and P. Sarcevic: A Comparison of Neural Networks and Fuzzy Inference Systems for the Identification of Magnetic Disturbances in Mobile Robot Localization, Acta Polytechnica Hungarica, Vol. 22, pp. 239-264, May 2025

[6] C. Storm, H. Hose, and R. H. Schmitt: State Estimation and Model-Predictive Control for Multi-Robot Handling and Tracking of AGV Motions using iGPS, in IEEE International Conference on Intelligent Robots and Systems, 2021

[7] M. Dares, K. W. Goh, Y. S. Koh, C. F. Yeong, E. L. M. Su, and P. H. Tan: Automated Guided Vehicle Robot Localization with Sensor Fusion, in Lecture Notes in Electrical Engineering, 2022

[8] J. Simon: Fuzzy Control of Self-Balancing, Two-Wheel-Driven, SLAM-Based, Unmanned System for Agriculture 4.0 Applications, Machines, Vol. 11, No. 4, 2023

[9] D. M. Lee and B. Labinghisa: Indoor localization system based on virtual access points with filtering schemes, Int J Distrib Sens Netw, Vol. 15, No. 7, 2019

[10] J. Huang, X. Yu, Y. Wang, and X. Xiao: An integrated wireless wearable sensor system for posture recognition and indoor localization, Sensors (Switzerland), Vol. 16, No. 11, 2016

[11] Y. Dobrev, S. Flores, and M. Vossiek: Multi-modal sensor fusion for indoor mobile robot pose estimation, in Proceedings of the IEEE/ION Position, Location and Navigation Symposium, PLANS 2016, 2016

[12] H. Ma and K. Wang: Fusion of RSS and Phase Shift Using the Kalman Filter for RFID Tracking, IEEE Sens J, Vol. 17, No. 11, 2017

[13] X. Shi, J. Tan, and D. Zhang: Indoor wheeled robot positioning algorithm based on extended kalman filter, in Proceedings - 2019 IEEE International Conferences on Ubiquitous Computing and Communications and Data Science and Computational Intelligence and Smart Computing, Networking and Services, IUCC/DSCI/SmartCNS 2019, 2019

[14] K. Tian, M. Radovnikovich, and K. C. Cheok: Comparing EKF, UKF, and PF Performance for Autonomous Vehicle Multi-Sensor Fusion and Tracking in Highway Scenario, in SysCon 2022 - 16th Annual IEEE International Systems Conference, Proceedings, 2022

[15] J. Kuti and P. Galambos: Modular C++ Library for Relaxed Unscented Kalman-Filtering, Acta Polytechnica Hungarica, Vol. 21, pp. 57-74, May 2024

[16] M. Sever, T. Y. Erkec, and C. Hajiyev: Comparison of EKF&UKF for GNSS Based Micro Satellite Orbital State Estimation, in Proceedings of 10th International Conference on Recent Advances in Air and Space Technologies, RAST 2023, 2023

[17] G. Kermarrec, A. Jain, and S. Schon: Kalman Filter and Correlated Measurement Noise: The Variance Inflation Factor, IEEE Trans Aerosp Electron Syst, Vol. 58, No. 2, 2022

[18] A. D. Sabiha, M. A. Kamel, E. Said, and W. M. Hussein: Real-time path planning for autonomous vehicle based on teaching–learning-based optimization, Intell Serv Robot, Vol. 15, No. 3, 2022

[19] L. Zhou, M. Wang, X. Zhang, P. Qin, and B. He: Adaptive SLAM Methodology Based on Simulated Annealing Particle Swarm Optimization for AUV Navigation, Electronics (Switzerland), Vol. 12, No. 11, 2023

[20] X. Mu, G. Yue, N. Zhou, and C. Chen: Occupancy Grid-Based AUV SLAM Method with Forward-Looking Sonar, J Mar Sci Eng, Vol. 10, No. 8, 2022

[21] S. László and Z. Vamossy: Improved RGB-D Camera-based SLAM System for Mobil Robots, Acta Polytechnica Hungarica, Vol. 21, pp. 107-124, May 2024

[22] M. Stefanoni, G. Fodor, P. Sarcevic, and Á. Odry: Evaluation of 2D Localization Performance in Wheeled Robots Based on the Fusion of Odometry and Absolute Positioning Systems, Budapest, May 2025